Current Research in Food Science 5 (2022) 752–762

Contents lists available at ScienceDirect

Current Research in Food Science

journal homepage: www.sciencedirect.com/journal/current-research-in-food-science

In vitro digestive characteristics and microbial degradation of polysaccharides from lotus leaves and related effects on the modulation of intestinal microbiota

Ding-Tao Wu [a,b,*], Kang-Lin Feng [a,b], Fen Li [b], Yi-Chen Hu [a], Sheng-Peng Wang [c], Ren-You Gan [a,d,**], Liang Zou [a,***]

[a] Key Laboratory of Coarse Cereal Processing, Ministry of Agriculture and Rural Affairs, Sichuan Engineering & Technology Research Center of Coarse Cereal Industralization, School of Food and Biological Engineering, Chengdu University, Chengdu, 610106, China
[b] Institute of Food Processing and Safety, College of Food Science, Sichuan Agricultural University, Ya'an, 625014, Sichuan, China
[c] State Key Laboratory of Quality Research in Chinese Medicine, Institute of Chinese Medical Sciences, University of Macau, Macao
[d] Research Center for Plants and Human Health, Institute of Urban Agriculture, Chinese Academy of Agricultural Sciences, Chengdu, 610213, China

ARTICLE INFO

Handling editor: Alejandro G. Marangoni

Keywords:
Lotus leaf
Polysaccharides
Structural characteristic
Digestive characteristic
Microbial degradation
Gut microbiota

ABSTRACT

Polysaccharides exist as one of the most abundant components in lotus leaves, which attract increasing attention owing to their promising health-promoting benefits. In this study, the digestive and microbial degradation characteristics of lotus leaf polysaccharides (LLP) were studied by using an *in vitro* gastrointestinal model. The results suggested that LLP was stable in the human upper gastrointestinal tract *in vitro* according to its digestive stabilities at different simulated digestion stages. Conversely, the indigestible LLP (LLPI) could be remarkably utilized by intestinal microbiota in human feces during *in vitro* fermentation, and its fermentability was 58.11% after the *in vitro* fermentation of 48 h. Indeed, the microbial degradation characteristics of LLPI during *in vitro* fermentation by human fecal inoculum were revealed. The results showed that the content of reducing sugars released from LLPI obviously increased from 0.498 to 2.176 mg/mL at the initial fermentation stage (0–6 h), and its molecular weight sharply decreased from 4.08×10^4 to 2.02×10^4 Da. Notably, the molar ratios of arabinose (Ara), galactose (Gal), and galacturonic acid (GalA) in LLPI decreased from 2.89 to 1.40, from 5.46 to 3.72, and from 21.24 to 18.71, respectively, suggesting that the utilization of arabinose and galactose in LLPI by intestinal microbiota was much faster than that of galacturonic acid at the initial fermentation stage. Additionally, LLPI could remarkably regulate gut microbial composition by increasing the abundances of several beneficial microbes, including *Bacteroides, Bifidobacterium, Megamonas,* and *Collinsella*, resulting in the promoted generation of several short-chain fatty acids, especially acetic, propionic, and butyric acids. The findings from the present study are beneficial to better understanding the digestive and microbial degradation characteristics of LLP, which indicate that LLP can be used as a potential prebiotic for the improvement of intestinal health.

1. Introduction

Lotus (*Nelumbo nucifera* Gaertn.), an aquatic plant of the family *Nelumbonaceae*, is widely cultivated as an industrial crop in eastern Asia, particularly in China (Chen et al., 2019a; Wang et al., 2021). Lotus is mainly consisted of leaf, flower, seed, and root. Among them, lotus leaves are usually consumed as herbal teas, diet drinks, beverages, and dishes, which also have a long history to be used as traditional medicines to prevent and treat diverse diseases, such as haematemesis, hyperlipidaemia, hypertension, epistaxis, and obesity (Chen et al., 2019a; Wang et al., 2021). Besides, lotus leaves have also attracted increasing attention for functional food development owing to their promising

* Corresponding author. Key Laboratory of Coarse Cereal Processing, Ministry of Agriculture and Rural Affairs, Sichuan Engineering & Technology Research Center of Coarse Cereal Industralization, School of Food and Biological Engineering, Chengdu University, Chengdu, 610106, China.
** Corresponding author. Key Laboratory of Coarse Cereal Processing, Ministry of Agriculture and Rural Affairs, Sichuan Engineering & Technology Research Center of Coarse Cereal Industralization, School of Food and Biological Engineering, Chengdu University, Chengdu, 610106, China.
*** Corresponding author.
E-mail addresses: wudingtao@cdu.edu.cn (D.-T. Wu), ganrenyou@yahoo.com (R.-Y. Gan), zouliang@cdu.edu.cn (L. Zou).

https://doi.org/10.1016/j.crfs.2022.04.004
Received 10 February 2022; Received in revised form 17 March 2022; Accepted 7 April 2022
Available online 21 April 2022

health benefits, including antioxidant, hypoglycemic, immunomodulatory, hepatoprotective, anti-proliferative, and anti-obesity effects, as well as modulation of colonic microbiota (Wang et al., 2020; Wang et al., 2021). Indeed, lots of studies have revealed that there are many bioactive components existing in lotus leaves, such as polysaccharides, polyphenols, flavonoids, and alkaloids, which contribute to their multiple health-promoting effects (Wang et al., 2021). Particularly, polysaccharides have been regarded as the most abundant components in the tea beverages of lotus leaves, ranging from about 3.22% to 6.31% (*w/w*) (Zhang et al., 2015; Wu et al., 2021a). The purified polysaccharides from lotus leaves have been reported to possess relatively low molecular weights ranging from about 12.5 kDa to 40.3 kDa (Song et al., 2019; Huang et al., 2021; Wu et al., 2021a). The major constituent monosaccharides in polysaccharides from louts leaves include galactose, galacturonic acid, arabinose, rhamnose, mannose, glucose, and glucuronic acid, indicating that homogalacturonan (HG), rhamnogalacturonan I (RG I), and arabinogalactan (AG) exist in lotus leaves (Huang et al., 2021; Wu et al., 2021a). Furthermore, these pectic polysaccharides from lotus leaves also possess diversely beneficial effects, such as antioxidant, anti-glycation, anti-cancer, anti-diabetic, and immunomodulatory effects (Huang et al., 2021; Li et al., 2021; Song et al., 2019; Wu et al., 2021a; Zeng et al., 2017; Zhang et al., 2015). Collectively, these studies suggest that lotus leaf polysaccharides (LLP) possess potential applications in the functional food industry.

The bioactivities of dietary polysaccharides are closely related to their digestive and microbial degradation characteristics from the stomach to the intestine (Guo et al., 2021). In fact, recent studies have demonstrated that the human gastrointestinal tract can be one of the most important loci for healthy performance of dietary polysaccharides (Xu et al., 2019; Zhang et al., 2020). Accumulating *in vitro* evidence has demonstrated that most of dietary polysaccharides are resistant to be digested in the human upper gastrointestinal tract owing to the lack of certain specific enzymes in human body, while these indigestible polysaccharides can enter into the colon and interact with the colonic bacteria (Guo et al., 2021). Generally, there are trillions of colonic bacteria colonizing in the human intestine, which provide the host with a range of beneficial functions, such as catabolism of complex dietary macronutrients, preventing against pathogen infection, and maintaining the immune system (Song et al., 2021). Notably, a large number of carbohydrate active enzymes encoded by the intestinal microbiota can degrade indigestible polysaccharides and their complexes into fermentable monosaccharides, which are in turn utilized by the intestinal microbiota, further exerting beneficial effects on the host (Koropatkin et al., 2012). Increasing studies have confirmed that different types of indigestible polysaccharides can modulate gut microbial composition by promoting the proliferation of beneficial intestinal microbes and reducing harmful intestinal bacteria, thereby improving the intestinal health (Kong et al., 2021; Li et al., 2020; Wu et al., 2021b; Wu et al., 2021c; Wu et al., 2021d). Moreover, the major metabolites of dietary polysaccharides utilized by specific intestinal microorganisms are short-chain fatty acids (SCFAs), which are the main energy sources for colonocytes and can also help prevent metabolic disorders, inflammatory bowel diseases, and related diseases (Fan and Pedersen, 2021). Therefore, the human intestinal microbiota can benefit from the fermentation and degradation of dietary polysaccharides. Nevertheless, the digestive characteristic and microbial degradation of LLP in the human gastrointestinal tract *in vitro* as well as related modulation effect on gut microbial composition have not yet been investigated.

In the present study, in order to reveal the potential digestive and microbial degradation characteristics of LLP, an *in vitro* simulated digestion and fecal fermentation model was applied to investigate the possible changes in LLP, as well as its regulation effect on the microbial composition. The findings from the present study will be helpful for understanding the digestive and microbial degradation characteristics of LLP, and beneficial to promoting the application of LLP as prebiotics in the functional food industry.

2. Materials and methods

2.1. Materials and chemicals

Lotus leaves (*Nelumbo nucifera* cv. Elian 6) were collected from Meishan, Sichuan Province, China. Inulin (INU), α-amylase (1000 U/mg), pancreatin (4000 U/g), and pepsin (3000 U/g) were obtained from Sigma-Aldrich (St. Louis, MO, USA) and Aladdin-E (Shanghai, China). Additionally, KCl, KH_2PO_4, $NaHCO_3$, NaCl, $MgCl_2(H_2O)_6$, $(NH_4)_2CO_3$, HCl, and $CaCl_2(H_2O)_2$ were obtained from Aladdin-E (Shanghai, China).

2.2. Preparation and isolation of LLP

Deep eutectic solvent (DES) assisted extraction was applied for the preparation of LLP as previously reported (Wu et al., 2021a). In brief, the extraction solvent was prepared by adding water into the DES (choline chloride: ethylene glycol = 1: 3, molar ratio) to maintain a solution ratio of 6: 4 (H_2O: DES, *v/v*). Furthermore, the sample powders (10.0 g) were firstly treated with 100 mL of ethanol (80%, *v/v*) for 2 h to remove small substances, such as phenolics and pigments. Then, the extracted residues were mixed with 300 mL of the DES extraction solvent for preparation of polysaccharides at 90 °C for 2 h. Finally, both graded alcohol precipitation and membrane separation were applied for the isolation of LLP in the extracted mixture. The extracted mixture (about 300 mL) was precipitated with 900 mL of ethanol (95%, *v/v*) to obtain crude polysaccharides. The crude polysaccharides were redissolved and further ultra-filtered (molar mass cutoff, 3.0 kDa) to remove impurities. Finally, LLP was obtained, and the yield was about 4.3%.

2.3. Simulated static digestion of LLP

An *in vitro* INFOGEST static digestion model with minor modifications was applied for the investigation of the digestive characteristics of LLP (Brodkorb et al., 2019), and the electrolyte solutions used for simulated salivary fluid (SSF), gastric fluid (SGF), and intestinal fluid (SIF) were also prepared according to the literature (Brodkorb et al., 2019). In the oral digestion phase, 100 mL of the SSF electrolyte solution and α-amylase (15000 U) were added into 100 mL of LLP solution (15 mg/mL), and digested in a water bath shaker at 37 °C. Then, at the digestion points of 15 min and 30 min, 2 mL of the digested solution was taken out and put into boiling water for 5 min before further analysis. After the oral digestion phase, 100 mL of the pre-warmed SGF electrolyte solution (37 °C) was mixed with 100 mL of the saliva digested sample, and the pH value was adjusted to 3.0 with 1 M HCl. Subsequently, the pepsin was added into the digestion mixture to achieve a final activity of 20 U/mL, and incubated at 37 °C. At the digestion points of 0.5 h, 1 h, and 2 h, 2 mL of the digested solution was also taken out and put it into boiling water for 5 min. In the intestinal digestion phase, 100 mL of pre-warmed SIF electrolyte solution (37 °C) was mixed with 100 mL of the gastric digested sample, and NaOH (1 M) was added into the mixture to adjust the pH to 7.0. Then, the pancreatin and bile salts were added into the mixture to reach final concentrations of 100 U/mL and 10 mM, respectively, and the mixture was incubated at 37 °C. At the digestion points of 0.5 h, 1 h, and 2 h, 2.0 mL of the digested solution was also taken out and put it into boiling water for 5 min. Finally, all digested mixtures collected at different digestion stages were sequentially treated by 95% of ethanol (three volumes), ultra-filtered (molar mass cutoff, 3.0 kDa), and freeze dried to get digested LLP samples, namely LLPS, LLPG, and LLPI, respectively.

2.4. Microbial fermentation of the indigestible LLP (LLPI) by human feces in vitro

An *in vitro* fermentation model was applied for the investigation of the microbial degradation characteristics of LLPI by human fecal microbiota as previously reported (Wu et al., 2021d). The basic culture

medium (1 L) was prepared as described in the literature (Wu et al., 2021d), which was composed of yeast extract, peptone, $NaHCO_3$, bile salts, NaCl, K_2HPO_4, KH_2PO_4, $CaCl_2(H_2O)_2$, $MgSO_4(H_2O)_7$, hemin, L-cysteine, resazurin solution, tween 80, and vitamin K. Then the basic culture medium was sterilized for 20 min at 121 °C. Fresh feces were provided by four healthy volunteers (two male and two females, 20–25 years old) without any treatment of antibiotics. Then, fresh feces were diluted to 10% (*w/v*) with 0.9% of saline (*w/v*). The human fecal inoculum (1 mL) was added into a sealed sterilized vial, and then 9 mL of the basic culture medium including 100 mg of LLPI (LLPI group) was added. At the same time, the basic culture medium adding with inulin (100 mg) was served as the positive control (INU group), and the negative control (BLANK group) only contained the human fecal inoculum and the basic culture medium. Finally, three groups were incubated at 37 °C for the anaerobic fermentation. Anaerobic condition was maintained throughout the *in vitro* fecal fermentation by using an anaerobic chamber (BPN-300CS, Being Instrument, Shanghai, China). All fermented samples at different fermentation points of 6, 12, 24, and 48 h were collected, and were sequentially treated by ethanol, ultra-filtered (3.0 kDa), and freeze dried to obtained fermented LLPI, namely LLPI-6h, LLPI-12 h, LLPI-24 h, and LLPI-48 h, respectively.

2.5. Determination of variations in physicochemical characteristics of lotus leaf polysaccharides during in vitro digestion and fermentation by human feces

2.5.1. Determination of reducing sugar contents (C_R), chemical compositions, and fermentabilities

The reducing sugars released from LLP were measured by the 3,5-dinitrosalicylic acid method as previously reported (Wu et al., 2021d). The *m*-hydroxydiphenyl and phenol-sulfuric acid methods were applied for the measurement of total uronic acids and total polysaccharides in LLP at different digested and fermented stages *in vitro* (Wu et al., 2021d), respectively. Furthermore, the fermentabilities (%) of LLPI at different fermented stages were calculated according to the contents of total sugars and reducing sugars (Wu et al., 2021d).

2.5.2. Measurement of molecular weights, monosaccharide compositions, and free monosaccharides released

Molecular weights of LLP at different digested and fermented stages *in vitro* were detected by using size exclusion chromatography. Both 18-angle laser light scattering detection and refractive index detection (Wyatt Technology Co., Santa Barbara, CA, USA) were used as formerly described (Wu et al., 2022). Additionally, the Shodex OHpak SB-806 M HQ (300 mm × 8.0 mm, i.d.) column was used. The monosaccharide compositions of LLP at different digested and fermented stages, as well as free monosaccharides released from LLPI at different fermented stages were determined by Ultimate U3000 LC system (Thermo Fisher Scientific, Waltham, MA, USA). A phenomenex gemini C18 110 A column (150 mm × 4.6 mm, 5 μm) was utilized for the separation of monosaccharides as previously reported (Yuan et al., 2019). Additionally, the mobile phase composed of a mixture of phosphate buffer solution (0.1 M, pH = 6.7) and acetonitrile (83: 17, *v/v*) was used.

2.5.3. Spectral analysis

The fourier transform infrared spectra (FT-IR) of LLP at different digested and fermented stages *in vitro* were recorded in the frequency range of 4000 - 500 cm^{-1} by a Nicolet iS 10 FT-IR (Thermo Fisher Scientific, Waltham, MA, USA) (Wu et al., 2022). Additionally, the esterification degree (DE) values of LLP at different digested and fermented stages were also calculated through the FT-IR absorption bands around 1744 cm^{-1} and 1611 cm^{-1} by a previously reported method (Wu et al., 2022).

2.5.4. Measurement of pH values and short-chain fatty acids (SCFAs)

The pH values of the fermented broths of LLPI, INULIN, and BLANK groups at different fermented points of 0, 6, 12, 24, and 48 h were detected immediately by a pH meter (RMD-H800, Remond Auto, Shanghai, China). In addition, the SCFAs produced in the LLPI, INULIN, and BLANK groups at different fermented points of 0, 6, 12, 24, and 48 h were also measured by an Agilent GC system (Agilent Technologies, Santa Clara, CA, USA). A HP-INNOWAX column (30 m × 0.25 mm × 0.25 μm) was applied for the separation of SCFAs as previously reported (Wu et al., 2021d). SCFA standards, including acetic, propionic, *i*-butyric, *n*-butyric, *i*-valeric, and *n*-valeric acids, were used to establish the calibration curves.

Table 1
Reducing sugar contents (C_R) of polysaccharides from lotus leaves during *in vitro* digestion and fermentation by human feces.

Digestion and fermentation processes	Time (h)	C_R (mg/mL)
Salivary digestion	0.25	0.112 ± 0.004 [a]
	0.5	0.114 ± 0.006 [a]
Gastric juice digestion	0.5	0.107 ± 0.006 [a]
	1	0.104 ± 0.005 [a]
	2	0.105 ± 0.004 [a]
	4	0.104 ± 0.005 [a]
Small intestinal juice digestion	0.5	0.094 ± 0.003 [a]
	1	0.096 ± 0.003 [a]
	2	0.092 ± 0.006 [a]
	4	0.097 ± 0.004 [a]
Fecal microbial fermentation	0	0.498 ± 0.022 [d]
	6	2.176 ± 0.028 [a]
	12	2.115 ± 0.080 [a]
	24	1.571 ± 0.064 [b]
	48	1.378 ± 0.037 [c]

Values represent mean ± standard deviation, and different superscript lowercase letters (a-d) indicate significance ($p < 0.05$) in each row. Statistical significances were carried out by ANOVA and Duncan's test.

2.6. Analysis of the microbial composition

After the *in vitro* fermentation by human feces for 48 h, the extraction, PCR amplification, purification, and sequencing of the bacterial 16 S rRNA genes of the fermented mixture were performed as previously reported (Wu et al., 2021b; Wu et al., 2021d). Besides, the gene sequencing data were also processed and analyzed as previously reported (Wu et al., 2021b; Wu et al., 2021d).

2.7. Statistical analysis

All data were expressed as means ± standard deviation. One-way analysis of variance (ANOVA) plus *post hoc* Duncan's test (SPSS software, version 24.0, IBM, Armonk, NY, USA) was applied for the evaluation of statistical significance. *P* value less than 0.05 was defined as statistical significance.

3. Results and discussion

3.1. Digestive characteristics of LLP in vitro

3.1.1. Digestive characteristics of C_R, molecular weights, and chemical compositions

Generally, the α-1,4-glycosidic linkages of soluble starch and some other α-polysaccharides can be degraded by α-amylase which exists in the upper gastrointestinal tract, resulting in the increase of reducing sugar contents (Wu et al., 2021d). Thus, the reducing sugars released from of LLP at different digested stages in the upper gastrointestinal tract *in vitro* were studied to reveal its digestive characteristics. The variation in C_R is presented in Table 1. Results showed that there were no significant variations in C_R of LLP after different digested stages, indicating that LLP was stable after the *in vitro* digestion. Additionally, as shown in Fig. 1A, a single polysaccharide fraction could be found in LLP,

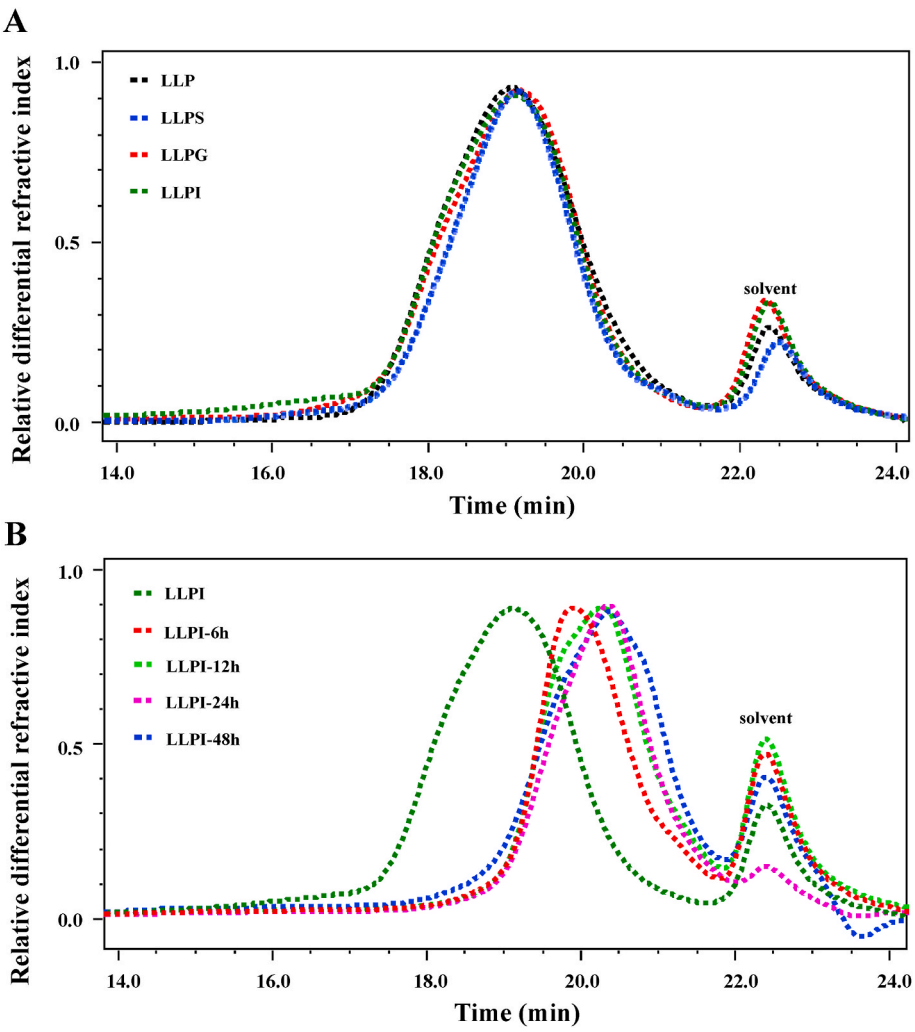

Fig. 1. Dynamic change in SEC chromatograms of LLP during *in vitro* digestion (A) and fermentation by human feces (B)
LLP, polysaccharides isolated from loquat leaves; **LLPS**, **LLPG,** and **LLPI** indicate LLP digested at different stages, including salivary, saliva-gastric, and saliva-gastrointestinal digestion stages, respectively; **LLP-6**, **LLP-12**, **LLP-24**, and **LLP-48** indicate human fecal fermentation of indigestible LLPI for 6, 12, 24, and 48 h, respectively.

Table 2
Changes in fermentability and chemical composition of polysaccharides from lotus leaves during *in vitro* digestion and fermentation by human feces.

	In vitro digestion of LLP				*In vitro* fermentation of LLPI			
	LLP	LLPS	LLPG	LLPI	LLPI-6	LLPI-12	LLPI-24	LLPI-48
Fermentability (%)	-	-	-	-	20.75 ± 1.36 ^{d}	30.23 ± 1.47 ^{c}	36.54 ± 1.85 ^{b}	58.11 ± 2.55 ^{a}
Total polysaccharides (%)	82.35 ± 1.48 ^{a}	79.91 ± 1.85 ^{a}	81.29 ± 2.38 ^{a}	80.10 ± 2.46 ^{a}	79.39 ± 1.47 ^{ab}	77.46 ± 2.12 ^{bc}	74.63 ± 0.89 ^{cd}	74.18 ± 1.17 ^{d}
Total uronic acids (%)	39.44 ± 1.27 ^{a}	39.65 ± 1.44 ^{a}	38.95 ± 1.42 ^{a}	39.03 ± 1.26 ^{a}	35.77 ± 0.80 ^{b}	34.84 ± 1.94 ^{b}	29.93 ± 1.50 ^{c}	28.23 ± 1.63 ^{c}
Degree of esterification (%)	28.68 ± 0.64 ^{a}	28.80 ± 0.36 ^{a}	27.75 ± 0.49 ^{a}	27.78 ± 1.39 ^{a}	2.29 ± 0.15 ^{b}	2.44 ± 0.23 ^{b}	2.73 ± 0.12 ^{b}	2.92 ± 0.32 ^{b}

Sample codes were the same as in Fig. 1.
Values represent mean ± standard deviation, and different superscript lowercase letters (a-d) indicated significance ($p < 0.05$) in each row; Statistical significances were carried out by ANOVA and Duncan's test.

LLPS, LLPG, and LLPI, and their SEC profiles and retention time were identical. In agreement with this, the molecular weights of LLP, LLPS, LLPG, and LLPI were almost the same, which were determined to be 4.09×10^4, 4.11×10^4, 4.06×10^4, and 4.08×10^4 Da, respectively, further confirming that LLP could not be digested in the upper gastrointestinal tract *in vitro*. The digestive characteristics of LLP's molecular weight was similar to the results of several previous studies, such as polysaccharides extracted from tamarind seed, Fuzhuan brick tea, and *Flammulina velutipes* (Chen et al., 2018b; Li et al., 2020; Su et al., 2019). Moreover, total polysaccharides and total uronic acids existing in LLP were detected to be 82.35% and 39.44%, respectively, which were in agreement with previously reported results (Li et al., 2021; Song et al., 2019; Wu et al., 2021a). After the *in vitro* digestion, total polysaccharides and uronic acids in LLP were basically unchanged (Table 2), which retained 79.91% - 81.29%, and 38.95% - 39.65%, respectively. Consequently, it was inferred that LLP was overall resistant to the simulated salivary, gastric, and small intestinal fluids.

3.1.2. Digestive characteristics of monosaccharide compositions and FT-IR spectra

The digestive characteristics of monosaccharide compositions and FT-IR spectra of LLP at different digested stages *in vitro* were also measured. As shown in Fig. 2A, the monosaccharide compositions of LLP at different digested stages in the upper gastrointestinal tract *in vitro* were nearly the same and consisted of galacturonic acid (GalA), galactose (Gal), arabinose (Ara), rhamnose (Rha), glucuronic acid (GlcA),

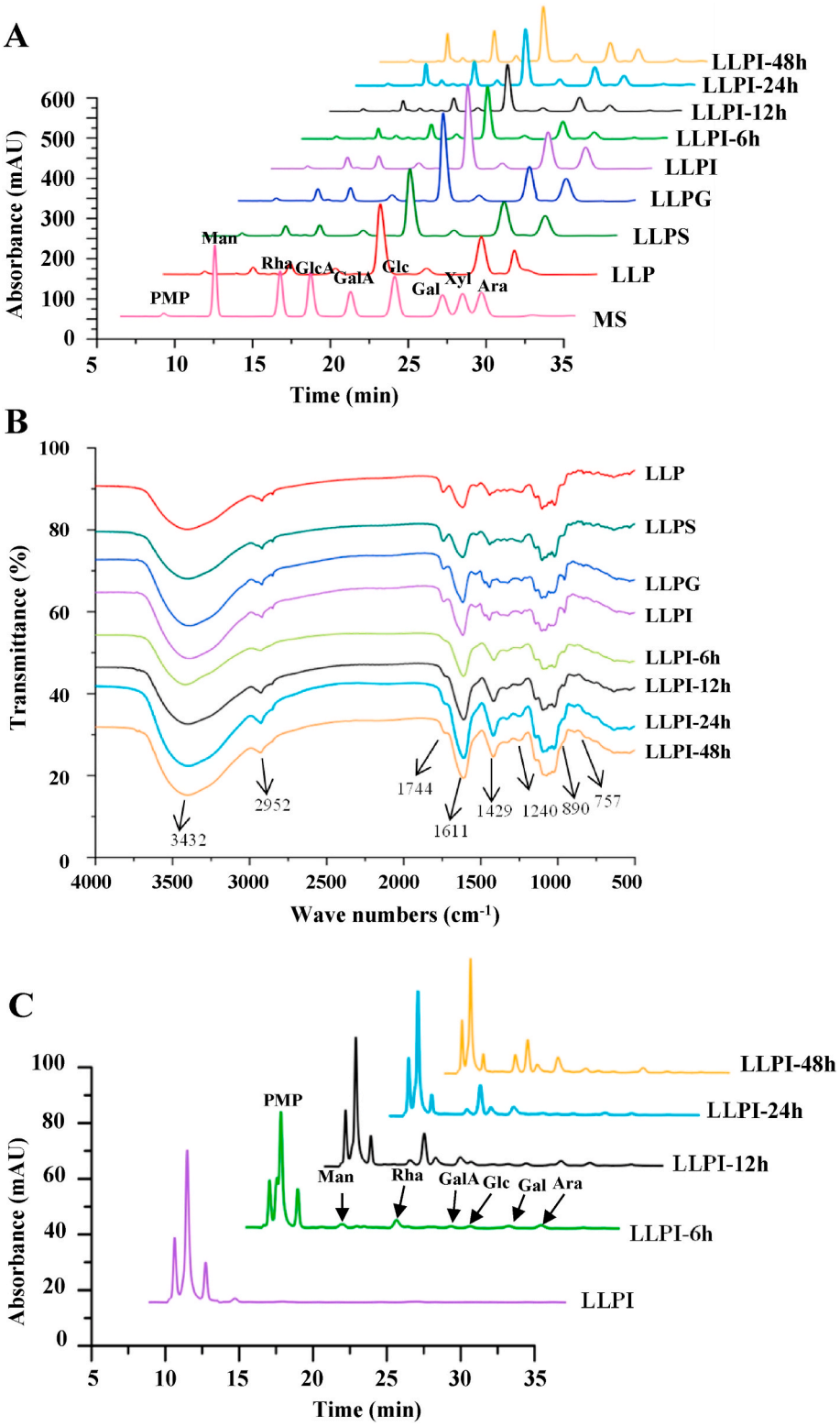

Fig. 2. Dynamic changes in constituent monosaccharides (A), FT-IR spectra (B), and free monosaccharides released (C) of LLP during *in vitro* digestion and fermentation by human fecesSample codes were the same as in Fig. 1. **PMP**, 1-phenyl-3-methyl-5-pyrazolone; **Man**, mannose; **Rha**, rhamnose; **GlcA**, glucuronic acid; **GalA**, galacturonic acid; **Glc**, glucose; **Gal**, galactose; **Xyl**, xylose; **Ara**, arabinose.

mannose (Man), and glucose (Glc). Also, the molar ratios of monosaccharides of LLP at different digested stages *in vitro* were almost the same, indicating that LLP was indigestible under the *in vitro* digestion conditions. GalA, Gal, Ara, and Rha existed as the main monosaccharides in all samples, suggesting that a high amount of homogalacturonan (HG) and arabinogalactan (AG) as well as a few of rhamnogalacturonan I (RG I) existed in LLP and its digested samples (Wu et al., 2021a). Moreover, the FT-IR spectra of LLP at different digested stages *in vitro* were also investigated to further reveal its digestive characteristics. As shown in Fig. 2B, the FT-IR spectra of LLP at different digested stages in the upper gastrointestinal tract *in vitro* were similar, indicating that the primarily chemical structure of LLP was overall stable. Additionally, the typical signals of acidic polysaccharides, including 3432, 2952, 1744, 1611, 1429, 1240, and 890 cm^{-1}, were

Table 3
Changes in constituent monosaccharides of polysaccharides from lotus leaves during *in vitro* digestion and fermentation by human feces.

	In vitro digestion of LLP				*In vitro* fermentation of LLPI			
	LLP	LLP-S	LLP-G	LLP-I	LLPI-6	LLPI-12	LLPI-24	LLPI-48
Constituent monosaccharides and molar ratios								
Man	1.14	1.12	1.09	1.16	1.20	1.23	2.79	3.13
Rha	1.59	1.65	1.56	1.55	2.13	2.14	4.70	5.15
GlcA	1.00	1.00	1.00	1.00	1.00	1.00	1.00	1.00
GalA	20.02	20.27	21.34	21.24	18.71	18.13	17.49	17.00
Glc	0.92	0.94	0.89	0.88	0.81	0.85	0.94	1.16
Gal	5.29	5.37	5.48	5.46	3.72	3.38	3.65	3.24
Ara	2.85	2.84	2.86	2.89	1.40	1.57	1.65	1.81

Sample codes were the same as in Fig. 1.

found in LLP and its digested samples (Li et al., 2021; Wu et al., 2021a). In addition, as shown in Table 1, the DE values of LLP, LLPS, LLPG, and LLPI were similar, which ranged from 27.75% to 28.80%. In summary, all abovementioned results indicated that LLP was stable at different digested stages in the upper gastrointestinal tract *in vitro*, and could arrive to the large intestine without any degradation for further fermentation by colonic bacteria.

3.2. Microbial degradation characteristics of the indigestible LLP (LLPI) by human fecal microbiota

3.2.1. Dynamic changes in chemical compositions and fermentabilities

The fermentabilities and chemical compositions of LLPI during the fermentation by human fecal inoculum are summarized in Table 2. The fermentabilities of LLPI-6h, LLPI-12 h, LLPI-24 h, and LLPI-48 h were measured to be 20.75%, 30.23%, 46.54%, and 58.11%, respectively, suggesting that the fermentation rate of LLPI was relatively fast at the initial fermentation stage (0–12 h). Besides, total polysaccharides and total uronic acids in LLPI remarkably decreased from 80.10% to 74.18% and from 39.03% to 28.23%, respectively, after the *in vitro* fermentation for 48 h. The results indicated that LLPI was utilized by colonic bacteria after the *in vitro* fecal fermentation. Generally, dietary polysaccharides can be degraded by different carbohydrate active enzymes produced by colonic microbes, such as *Bacteroides thetaiotaomicron* and *Bacteroides caccae* (Koropatkin et al., 2012).

3.2.2. Dynamic changes in C_R, free monosaccharides released, and molecular weights

The indigestible polysaccharides are easily broken down and utilized by intestinal microbiota to generate reducing sugars, which can be in turn utilized by gut bacteria (Wu et al., 2021d). Consequently, for evaluating the relationship between the depolymerization of polysaccharides and the growth of colonic bacteria during the fermentation, the reducing sugars released from LLPI were detected. As shown in Table 1, the C_R in the fermented broth of LLPI significantly increased from 0.498 mg/mL to 2.115 mg/mL at the initial fermentation stage (0–12 h), and then remarkably declined from 2.115 mg/mL to 1.571 mg/mL with the fermentation time increased (12–24 h). These results indicated that the degradation of LLPI by intestinal microbiota was predominant at the initial fermentation stage (0–12 h), and then the utilization of reducing sugars by intestinal microbiota was faster than the production of reducing sugars with the increasing fermentation time, thereby resulting in the decease of reducing sugar contents (Kong et al., 2021; Wu et al., 2021b; Wu et al., 2021d). Moreover, free sugars released from LLPI during *in vitro* fermentation were also analyzed, and results are shown in Fig. 2C. After the *in vitro* fermentation for 6 h, six monosaccharides, including Man, Rha, GalA, Glc, Gal, and Ara, were detected in the fermented broth of LLPI, suggesting that LLPI was degraded by intestinal microbiota. This result might be owing to some intestinal microbiota, such as *Bacteroides*, *Firmicutes*, and *Bifidobacterium*, which could degrade certain glycans (Chen et al., 2019b). In addition, the responses of several monosaccharides gradually decreased with the increasing fermentation time, indicating that the intestinal microbiota consumed free monosaccharides.

Furthermore, the change in molecular weights of LLPI was also determined to reveal its microbial degradation characteristics by intestinal microbiota during *in vitro* fermentation. As shown in Fig. 1B, the SEC profiles of LLPI at different fermented stages *in vitro* obviously shifted to right with the increase of retention time. More specifically, the SEC profile of LLPI notably shifted to right at the initial fermentation stage, indicating that LLPI was obviously degraded by intestinal microbiota during the fermentation process. In fact, the molecular weight of LLPI after the *in vitro* fermentation sharply decreased from 4.08×10^4 Da to 1.37×10^4 Da. More specifically, the molecular weights of LLPI-6h, LLPI-12 h, LLPI-24 h, and LLPI-48 were detected to be 2.02×10^4 Da, 1.77×10^4 Da, 1.67×10^4 Da, and 1.37×10^4 Da, respectively, suggesting that LLPI might be quickly degraded by intestinal microbiota into small fragments at the initial fermentation stage. Additionally, taken together with the result of reducing sugars (Table 1), it could indicate that the decrease of molecular weight of LLPI at different fermented stages *in vitro* may be primarily due to the breakdown of its glycosidic linkages (Wu et al., 2021b).

3.2.3. Dynamic changes in monosaccharide compositions and FT-IR spectra

Dietary polysaccharides can be degraded by intestinal microbiota, such as *Bacteroides thetaiotaomicron* and *Bacteroides caccae* (Koropatkin et al., 2012), resulting in the change of monosaccharide compositions (Guo et al., 2021). Hence, in the present study, the dynamic change in monosaccharide compositions of LLPI during *in vitro* fermentation by human feces was determined to further reveal its microbial degradation characteristics. As shown in Fig. 2A, the types of constituent monosaccharides of LLPI and its fermented samples were identical, composing of GalA, Gal, Ara, Rha, Man, Glc, and GlcA. Conversely, the molar ratios of monosaccharides in LLPI at different fermented stages *in vitro* remarkably changed (Table 3). More specifically, the molar ratios of Gal and Ara in LLPI notably decreased from 5.46 to 3.72 and from 2.89 to 1.40, respectively, after the *in vitro* fermentation for 6 h, indicating that the AG existing in LLPI might be quickly utilized by intestinal microbiota at the initial fermentation stage (Ding et al., 2019). Besides, the molar ratio of GalA also remarkably declined with the increasing fermentation time, while the molar ratio of Rha gradually increased, suggesting that the HG existing in LLPI might be also quickly utilized by intestinal microbiota during *in vitro* fermentation. Taken together with the result of free monosaccharides released (Fig. 2C), it could be presumed that the AG existing in LLPI might be more easily to be utilized by colonic bacteria than that of the backbones of HG and RG I.

Furthermore, the change in FT-IR spectra of LLPI at different fermented stages *in vitro* was also studied to reveal its microbial degradation characteristics. As shown in Fig. 2B, the typical signals of acidic polysaccharides, including 3432, 2952, 1744, 1611, 1429, 1240, and 890 cm^{-1}, were also found in LLPI and its fermented samples (Li et al., 2021; Wu et al., 2021a). Indeed, the FT-IR spectra of LLPI and its fermented samples (LLPI-6, LLPI-12, LLPI-24, and LLPI-48) at different fermentation stages *in vitro* were also similar, suggesting that the

Table 4
Changes in pH values and contents of short-chain fatty acids produced at different time points of fermentation.

Groups	Time (h)	pH	Short-chain fatty acids (mmol/L)						
			Acetic acid	Propionic acid	i-Butyric acid	n-Butyric acid	i-Valeric acid	n-Valeric acid	Total
BLANK	0	8.95 ± 0.01 a, B	ND	ND	ND	ND	ND	ND	ND
	6	8.73 ± 0.02 b, A	5.189 ± 0.004 d, B	ND	ND	ND	ND	ND	5.189 ± 0.004 c, C
	12	8.60 ± 0.02 c, A	6.095 ± 0.094 c, C	1.502 ± 0.113 a, B	0.286 ± 0.016 b, B	0.687 ± 0.025 c, B	0.488 ± 0.026 a, A	0.786 ± 0.054 b, B	9.877 ± 0.064 b, C
	24	8.14 ± 0.02 d, A	6.453 ± 0.045 b, C	1.698 ± 0.065 a, A	0.280 ± 0.005 b, B	0.784 ± 0.002 b, B	0.524 ± 0.024 a, A	0.867 ± 0.059 b, B	10.605 ± 0.019 a, B
	48	7.86 ± 0.02 e, A	6.731 ± 0.027 a, C	1.723 ± 0.002 a, B	0.367 ± 0.022 a, B	0.857 ± 0.029 a, B	0.275 ± 0.003 b, C	1.020 ± 0.007 a, B	10.702 ± 0.033 a, C
INU	0	9.11 ± 0.03 a, A	ND	ND	ND	ND	ND	ND	ND
	6	7.46 ± 0.04 b, B	6.266 ± 0.156 c, A	1.701 ± 0.078 c, A	0.291 ± 0.006 d, A	0.802 ± 0.016 bc, A	0.371 ± 0.040 a, A	1.226 ± 0.083 a, A	10.657 ± 0.024 d, A
	12	6.82 ± 0.01 c, B	7.267 ± 0.030 b, B	1.621 ± 0.007 c, AB	0.368 ± 0.004 c, A	0.775 ± 0.009 c, AB	0.344 ± 0.009 a, B	1.233 ± 0.016 a, A	11.606 ± 0.021 c, A
	24	5.88 ± 0.04 d, B	7.973 ± 0.015 b, B	1.845 ± 0.027 b, A	0.429 ± 0.015 b, A	0.844 ± 0.014 a, A	0.312 ± 0.006 a, B	1.216 ± 0.125 a, A	12.619 ± 0.171 b, A
	48	5.19 ± 0.02 e, B	8.667 ± 0.031 a, B	2.356 ± 0.044 a, A	0.781 ± 0.037 a, A	0.809 ± 0.002 b, B	0.349 ± 0.010 a, B	1.134 ± 0.029 a, A	14.096 ± 0.141 a, B
LLPI	0	8.21 ± 0.02 a, C	ND	ND	ND	ND	ND	ND	ND
	6	7.16 ± 0.06 b, C	6.447 ± 0.042 d, A	1.716 ± 0.010 b, A	0.251 ± 0.014 b, B	0.746 ± 0.020 b, B	0.246 ± 0.003 b, B	0.683 ± 0.023 a, B	10.088 ± 0.028 d, B
	12	6.23 ± 0.03 c, C	7.845 ± 0.070 c, A	1.731 ± 0.032 b, A	0.246 ± 0.017 b, B	0.744 ± 0.022 b, A	0.257 ± 0.037 b, C	0.675 ± 0.004 a, C	11.499 ± 0.031 c, B
	24	5.47 ± 0.04 d, C	8.540 ± 0.404 b, A	1.805 ± 0.039 b, A	0.244 ± 0.012 b, B	0.759 ± 0.003 b, B	0.241 ± 0.008 b, C	0.677 ± 0.026 a, B	12.265 ± 0.321 b, A
	48	4.94 ± 0.01 e, C	9.940 ± 0.099 a, A	2.534 ± 0.202 a, A	0.662 ± 0.263 a, A	0.985 ± 0.027 a, A	0.379 ± 0.005 a, A	0.706 ± 0.021 a, C	15.206 ± 0.377 a, A

Sample codes were the same as in Fig. 3. Values represent mean ± standard deviation, and different capital letters (A-C) showed significant differences among different groups ($p < 0.05$) at the same time point, while lowercase letters (a-e) represented significant differences among different time ($p < 0.05$) in the same group; Statistical significances were carried out by ANOVA and Duncan's test. ND: not detected.

primary structure of LLPI was still relatively stable. Conversely, the intensity of the signal at 1744 cm^{-1} obviously decreased, indicating that the esterified groups of LLPI were degraded. The DE values of LLPI obviously decreased from 27.78% to 2.92% after the *in vitro* fermentation for 48 h. This result might be due to that some intestinal microbiota could produce certain enzymes to degrade the esterified groups of LLPI (Koropatkin et al., 2012).

3.2.4. Dynamic changes in pH values and SCFAs

The change in pH values can reflect the fermentation degree of dietary polysaccharides during *in vitro* fermentation (Day et al., 2012). As shown in Table 4, the pH values in the experimental group (LLPI), negative control group (BLANK), and positive control group (INU) obviously changed after the *in vitro* fermentation. More specifically, the pH values of the negative control group slightly decreased from 8.95 to 7.86 at the end of the fermentation stage. However, a rapid and significant decrease in pH values was observed in the experimental group, which declined from 8.21 to 4.94. Besides, the pH values of the positive control group also declined notably from 9.11 to 5.19. After the *in vitro* fermentation for 48 h, the pH values of the experimental group and the positive control group were obviously lower than that of the negative control group, indicating that the addition of LLPI and inulin in the fermentation medium could generate lots of acidic metabolites (Kong et al., 2021). Indeed, studies have shown that a weakly acidic environment can improve the proliferation of beneficial microbes in the intestine and inhibit the growth of harmful microbes (Slavin, 2013). Therefore, LLPI may have a physiological role in promoting intestinal health.

The major metabolites of dietary polysaccharides utilized by intestinal microbiota during *in vitro* fermentation are short-chain fatty acids (SCFAs), which play key roles in the intestinal health (Nicholson et al., 2012). So, in the present study, the change in SCFAs produced by colonic microbiota during *in vitro* fermentation was measured. Six different SCFAs, including acetic, propionic, *n*-butyric, *i*-butyric, *n*-valeric, and *i*-valeric acids, were determined. The contents of SCFAs produced at different fermented stages in the BLANK, LLPI, and INU groups are summarized in Table 4. In the experimental group (LLPI), the concentration of total SCFAs increased significantly ($p < 0.05$) to 15.206 mmol/L at the end stage of fermentation process, which was obviously higher than that of the negative control group (BLANK, 10.702 mmol/L) and the positive control group (INU, 14.096 mmol/L) group. Usually, acetic acid is the major SCFA in the intestine, which is absorbed by the colonic epithelium and transported to target tissues and organs, such as brain, heart, and nerve tissues, as the energy (Koh et al., 2016). After the *in vitro* fermentation, the concentrations of acetic acid in the BLANK, INU, and LLPI groups reached 6.731, 8.667, and 9.940 mmol/L, respectively. Additionally, propionic acid can relieve the intestinal immune stress and plays an important role in the homeostasis of the intestinal environment (van der Beek et al., 2017). In the present study, the concentrations of propionic acid in the BLANK, INU, and LLPI groups reached 1.723, 2.356, and 2.534 mmol/L, respectively. Moreover, butyric acid is an energy source for intestinal epithelial cells with anti-inflammatory and anti-cancer effects (Canani et al., 2011). The concentrations of *i*-butyric acid in the BLANK, INU, and LLPI groups at the end stage of fermentation process were 0.367, 0.781, and 0.662 mmol/L, respectively, while the concentrations of *n*-butyric acid were 0.857, 0.809, and 0.985 mmol/L, respectively. The high level of *n*-butyric acid detected in the experimental group (LLPI group) was probably owing to the enhancement of *Firmicutes* (Fu et al., 2019). The butyric, propionic, and acetic acids were the major metabolites of LLPI after the *in vitro* fermentation, and their levels produced were close to those of the INU group and higher than those of the BLANK group. These results indicated that LLPI could be utilized as a potential prebiotic by promoting the generation of SCFAs.

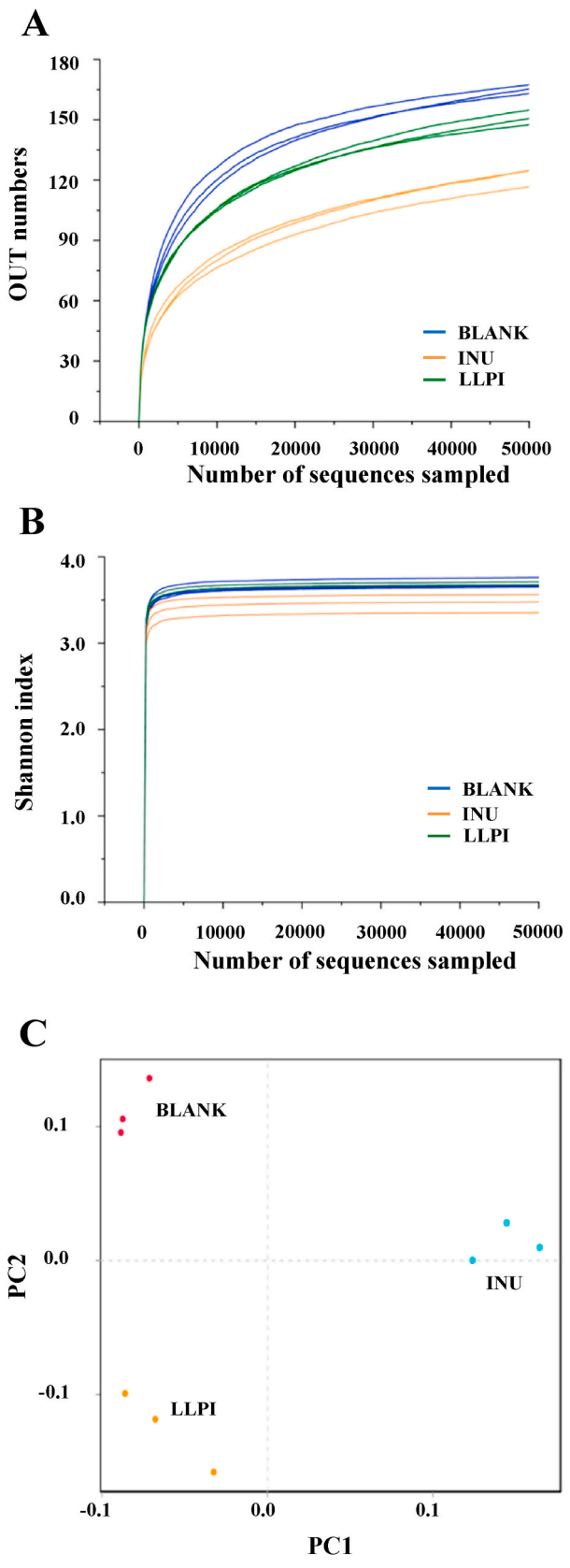

Fig. 3. Rarefaction curves (A), Shannon indexes (B), and principal coordinate analysis (C) of gut microbiota of the samples after the *in vitro* fermentation **BLANK**, the blank control (no additional carbon source supplement); **INU**, the positive control (INU supplement); **LLPI**, the experimental group (LLPI supplement).

3.3. Effect of the indigestible LLP (LLPI) on gut microbial composition

In the present study, the modulation effect of LLPI on gut microbial composition was studied by the 16 S rRNA gene pyrosequencing. Generally, the α-diversity is applied for the determination of the abundance of species and diversity in the community ecology (Chen et al., 2019b). As Fig. 3A displayed, the flat rarefaction curves were observed, indicating that the suitable sequencing data was collected in the present study. In addition, the Shannon indexes reached the plateau with the increasing read number, indicating that the data could represent most of the microbial information (Fig. 3B). Furthermore, the principal coordinate analysis (PCoA) was performed to reveal the β-diversity of tested samples. As shown in Fig. 3C, there was a distinct separation among the three groups, suggesting that the microbial community structure was different among the three groups.

The microbial compositions of three groups were analyzed at the phylum level in Fig. 4A, and the dominant compositions of LLPI and INU groups were *Firmicutes*, *Bacteroidetes*, *Actinobacteria,* and *Proteobacteria*. However, *Fusobacteria* which existed as the main bacteria in the BLANK group (34.76%) was almost inhibited in the LLPI and INU groups. It has been reported that *Fusobacteria* is generally considered as a conditional pathogen (Xu et al., 2020). Besides, the relative abundances of *Firmicutes* in both LLPI and INU groups were increased by 31.99% and 4.78%, respectively. Usually, several *Firmicutes* in the colon can generate SCFAs by fermenting dietary polysaccharides, thereby exerting a beneficial effect on the host. The acidic condition might be beneficial for the proliferation of butyrate-producing *Firmicutes* (Li et al., 2020). In addition, the relative abundance of *Bacteroidetes* in the LLPI group also obviously increased. Generally, dietary polysaccharides can be degraded by *Bacteroidetes*, such as *Bacteroides thetaiotaomicron* and *B. caccae*, which can generate lots of carbohydrate active enzymes (Koropatkin et al., 2012). Moreover, the relative abundance of *Actinobacteria* also notably increased in the LLPI group and INU group, which might be mainly attributed to the increase of *Bifidobacterium*. Generally, *Bifidobacterium* is identified as one of the important probiotics in the human gut, which can protect from enteropathogenic infection in the host through production of acetate (Fukuda et al., 2011). Furthermore, the relative abundance of *Proteobacteria* remarkably increased in the INU group but obviously decreased in the LLPI group. Generally, the proliferation of *Proteobacteria* can induce the imbalance of intestinal microbiota and low-grade inflammation, while it always exists in the feces of healthy human (Huang et al., 2020). Nevertheless, the abundances of *Fusobacteria* and *Proteobacteria* in the LLPI group (16.99%) were obviously lower than that of the INU group (68.56%) and the BLANK group (73.34%). Results indicated that the supplement of LLPI could modulate gut microbial composition by promoting the proliferation of beneficial microbiota.

At the genus level, Fig. 4B displays the intestinal bacteria distributions in different groups. The negative control group (BLANK) was mainly consisted of *Fusobacterium*, *uncultured_bacterium_f_Enterobacteriaceae*, *Escherichia-Shigella*, *Bacteroides*, *Bilophila*, and *Phascolarctobacterium,* which was similar to a previous study (Wu et al., 2021b). Compared with the negative control group, the abundances of some beneficial microbiota, such as *Bacteroides, Bifidobacterium, Megamonas,* and *Collinsella* in the LLPI group remarkably increased. *Bacteroides* is considered as one of the important gut microbiota to hydrolyze indigestible carbohydrates, and the increase of *Bacteroides* is beneficial for the prevention of obesity (Chen et al., 2018a; Chen et al., 2021). Besides, studies indicated that the proliferation of *Megamonas* could suppress the growth of harmful bacteria by competing energy intake (Gong et al., 2019). Conversely, in the LLPI group, the abundances of some harmful microbes, including *Fusobacterium* and *uncultured_bacterium_f_Enterobacteriaceae*, obviously decreased. It has been reported that *Fusobacterium* may be closely associated with the gastric oncogenesis (Han et al., 2020). In addition, the abundances of *Fusobacterium* and *Escherichia--Shigella* in the LLPI group (10.59%) also notably decreased, compared

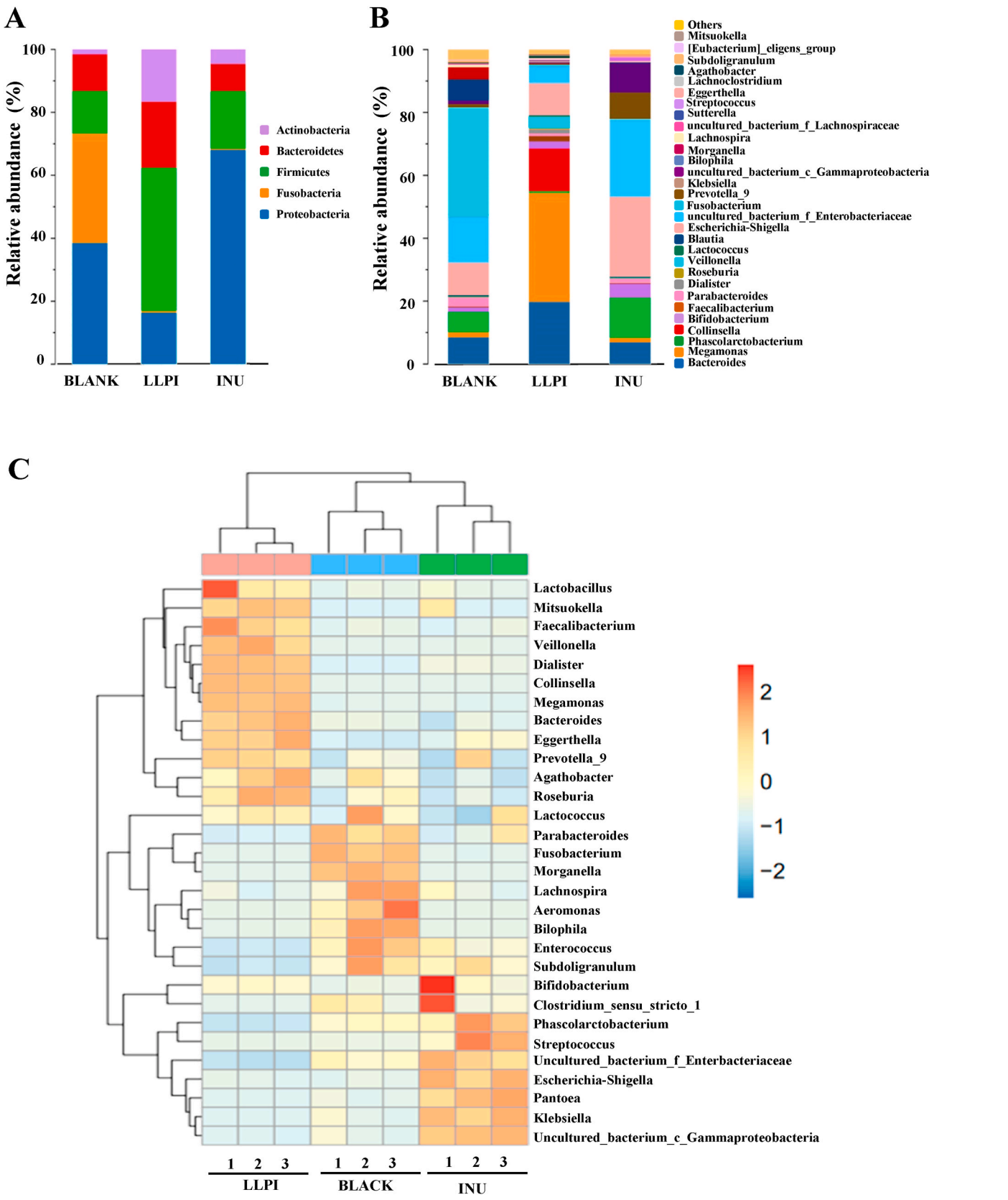

Fig. 4. The relative abundance of bacterial community at the phylum level (A) and at the genus level (B) as well as the heat map analysis of the relative abundance of bacterial community at the genus level (C)
Sample codes were the same as in Fig. 3.

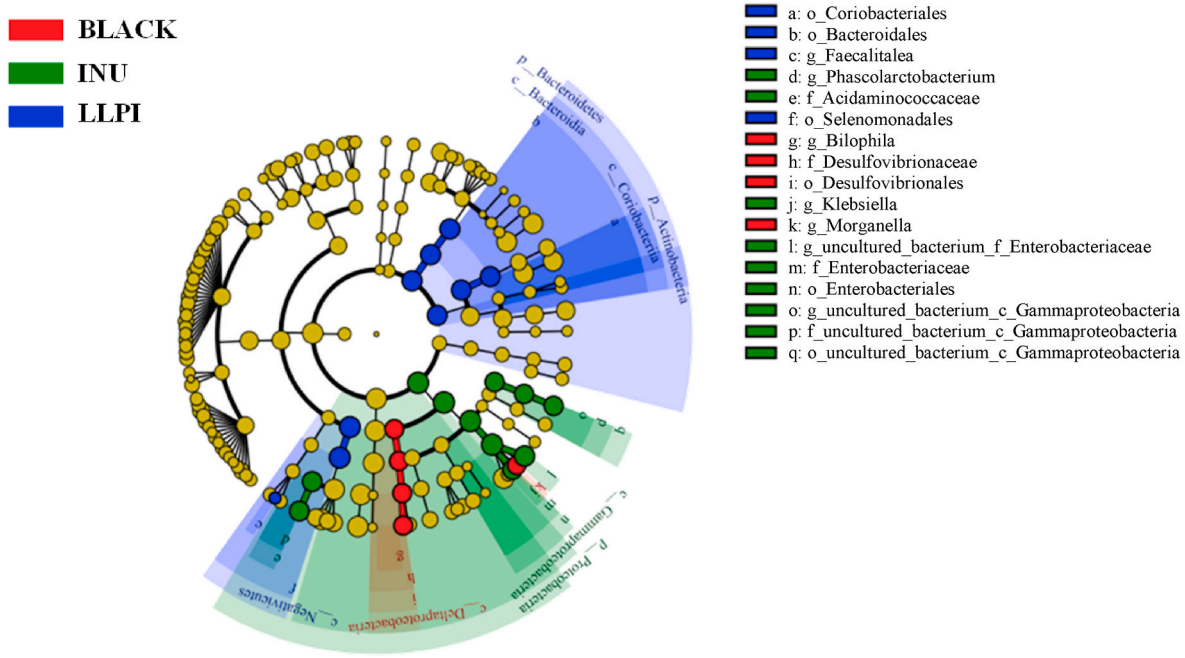

Fig. 5. Comparison of microbiota among BLANK, INU, and LLPI groups based on linear discriminant analysis effect size (LEfSe)
Sample codes were the same as in Fig. 3.

with the negative control group (44.98%). Furthermore, the INU group exhibited a higher abundance of *Phascolarctobacterium* and *Bifidobacterium* than that of the negative control group. It is reported that the enhancement of generation of SCFAs may be owing to the proliferation of *Bifidobacterium*. Besides, *Phascolarctobacterium* is also beneficial for anti-obesity effect (Chen et al., 2019b; Han et al., 2020). Meanwhile, the abundances of *Fusobacterium* and *Escherichia-Shigella* in the INU group (25.65%) were also lower than that of the negative control group (44.98%).

The heat map analysis is displayed in Fig. 4C. The results showed that the relative abundances of *Lactobacillus*, *Megamonas*, *Faecalibacterium*, *Veillonella, Dialister*, *Collinsella, Bacteroides*, and *Prevotella_9* were obviously promoted in the LLPI group when compared with the negative control group, while the relative abundance of *Morganella, Lachnospira, Aeromonas, Bilophila, Enterococcus, Subdoligranulum,* and *Fusobacterium* notably decreased. As shown in Fig. 5, *Coriobacteriales*, *Bacteroidales*, *Faecalitalea*, and *Selenomonadales* were in absolute dominance in LLPI group when compared with the negative control group. These results indicated that the supplement of LLPI could notably change gut microbial composition.

4. Conclusion

In conclusion, this study revealed that LLP was indigestible in the upper gastrointestinal tract *in vitro*, and could be fermented by the intestinal bacteria in the large intestine. The microbial degradation characteristics of the indigestible LLP (LLPI) were revealed. Notably, the AG fraction existed in LLPI might be more easily to be utilized by colonic bacteria than that of the backbones of HG and RG I at the initial stage of *in vitro* fermentation. Furthermore, LLPI could regulate gut microbial composition after the *in vitro* fermentation by promoting the proliferation of some beneficial microbes, such as genera *Bacteroides, Bifidobacterium, Megamonas,* and *Collinsella*, resulting in the generation of beneficial SCFAs. Results from this study are beneficial to understanding the potential digestive and microbial degradation characteristics of LLP, and LLP can be used as a potential prebiotic for promoting intestinal health.

CRediT authorship contribution statement

Ding-Tao Wu: Data curation, Methodology, Formal analysis, Funding acquisition, Writing – original draft. **Kang-Lin Feng:** Investigation, Formal analysis, Resources, Software. **Fen Li:** Investigation, Formal analysis, Validation. **Yi-Chen Hu:** Resources, Software. **Sheng-Peng Wang:** Resources, Software. **Ren-You Gan:** Formal analysis, Supervision, Funding acquisition, Writing – review & editing. **Liang Zou:** Methodology, Formal analysis, Supervision, Resources, Writing – review & editing.

Declaration of competing interest

The authors declare that they have no known competing financial interests or personal relationships that could have appeared to influence the work reported in this paper.

Acknowledgments

This work was supported by the Scientific Research Foundation of Chengdu University (No. 2081921047), the opening fund of the State Key Laboratory of Quality Research in Chinese Medicine, University of Macau (No. QRCM-OP21001), and the Opening Fund of the Key Laboratory of Coarse Cereal Processing, Ministry of Agriculture and Rural Affairs, Chengdu University (No. 2021CC002).

References

Brodkorb, A., Egger, L., Alminger, M., Alvito, P., Assuncao, R., Ballance, S., Bohn, T., Bourlieu-Lacanal, C., Boutrou, R., Carriere, F., Clemente, A., Corredig, M., Dupont, D., Dufour, C., Edwards, C., Golding, M., Karakaya, S., Kirkhus, B., Le Feunteun, S., Lesmes, U., Macierzanka, A., Mackie, A.R., Martins, C., Marze, S., McClements, D.J., Menard, O., Minekus, M., Portmann, R., Santos, C.N., Souchon, I., Singh, R.P., Vegarud, G.E., Wickham, M.S.J., Weitschies, W., Recio, I., 2019. INFOGEST static *in vitro* simulation of gastrointestinal food digestion. Nat. Protoc. 14 (4), 991–1014. https://doi.org/10.1038/s41596-018-0119-1.

Canani, R.B., Costanzo, M.D., Leone, L., Pedata, M., Meli, R., Calignano, A., 2011. Potential beneficial effects of butyrate in intestinal and extraintestinal diseases. World J. Gastroenterol. 17 (12), 1519–1528. https://doi.org/10.3748/wjg.v17.i12.1519.

Chen, G., Xie, M., Wan, P., Chen, D., Dai, Z., Ye, H., Hu, B., Zeng, X., Liu, Z., 2018a. Fuzhuan brick tea polysaccharides attenuate metabolic syndrome in high-fat diet induced mice in association with modulation in the gut microbiota. J. Agric. Food Chem. 66 (11), 2783–2795. https://doi.org/10.1021/acs.jafc.8b00296.

Chen, G., Xie, M., Wan, P., Chen, D., Ye, H., Chen, L., Zeng, X., Liu, Z., 2018b. Digestion under saliva, simulated gastric and small intestinal conditions and fermentation *in vitro* by human intestinal microbiota of polysaccharides from Fuzhuan brick tea. Food Chem. 244, 331–339. https://doi.org/10.1016/j.foodchem.2017.10.074.

Chen, G.L., Zhu, M.Z., Guo, M.Q., 2019a. Research advances in traditional and modern use of *Nelumbo nucifera*: phytochemicals, health promoting activities and beyond. Crit. Rev. Food Sci. Nutr. 59, S189–S209. https://doi.org/10.1080/10408398.2018.1553846.

Chen, L., Liu, J., Ge, X., Xu, W., Chen, Y., Li, F., Cheng, D., Shao, R., 2019b. Simulated digestion and fermentation *in vitro* by human gut microbiota of polysaccharides from *Helicteres angustifolia* L. Int. J. Biol. Macromol. 141, 1065–1071. https://doi.org/10.1016/j.ijbiomac.2019.09.073.

Chen, P., Chen, X.Q., Hao, L.L., Du, P., Li, C., Han, H.Y., Xu, H.X., Liu, L.B., 2021. The bioavailability of soybean polysaccharides and their metabolites on gut microbiota in the simulator of the human intestinal microbial ecosystem (SHIME). Food Chem. 362, 130233 https://doi.org/10.1016/j.foodchem.2021.130233.

Day, L., Gomez, J., Oiseth, S.K., Gidley, M.J., Williams, B.A., 2012. Faster fermentation of cooked carrot cell clusters compared to cell wall fragments *in vitro* by porcine feces. J. Agric. Food Chem. 60 (12), 3282–3290. https://doi.org/10.1021/jf204974s.

Ding, Y., Yan, Y., Peng, Y., Chen, D., Mi, J., Lu, L., Luo, Q., Li, X., Zeng, X., Cao, Y., 2019. *In vitro* digestion under simulated saliva, gastric and small intestinal conditions and fermentation by human gut microbiota of polysaccharides from the fruits of *Lycium barbarum*. Int. J. Biol. Macromol. 125, 751–760. https://doi.org/10.1016/j.ijbiomac.2018.12.081.

Fan, Y., Pedersen, O., 2021. Gut microbiota in human metabolic health and disease. Nat. Rev. Microbiol. 19 (1), 55–71. https://doi.org/10.1038/s41579-020-0433-9.

Fu, X., Liu, Z., Zhu, C., Mou, H., Kong, Q., 2019. Nondigestible carbohydrates, butyrate, and butyrate-producing bacteria. Crit. Rev. Food Sci. Nutr. 59 (Suppl. 1), S130–S152. https://doi.org/10.1080/10408398.2018.1542587.

Fukuda, S., Toh, H., Hase, K., Oshima, K., Nakanishi, Y., Yoshimura, K., Tobe, T., Clarke, J.M., Topping, D.L., Suzuki, T., Taylor, T.D., Itoh, K., Kikuchi, J., Morita, H., Hattori, M., Ohno, H., 2011. *Bifidobacteria* can protect from enteropathogenic infection through production of acetate. Nature 469 (7331), 543–547. https://doi.org/10.1038/nature09646.

Gong, L.X., Wang, H.N., Wang, T.X., Liu, Y.L., Wang, J., Sun, B.G., 2019. Feruloylated oligosaccharides modulate the gut microbiota *in vitro* via the combined actions of oligosaccharides and ferulic acid. J. Funct.Foods 60, 103453. https://doi.org/10.1016/j.jff.2019.103453.

Guo, Y.X., Chen, X.F., Gong, P., Chen, F.X., Cui, D.D., Wang, M.R., 2021. Advances in the *in vitro* digestion and fermentation of polysaccharides. Int. J. Food Sci. Tech. 56 (10), 4970–4982. https://doi.org/10.1111/ijfs.15308.

Han, R., Pang, D., Wen, L., You, L., Huang, R., Kulikouskaya, V., 2020. *In vitro* digestibility and prebiotic activities of a sulfated polysaccharide from *Gracilaria Lemaneiformis*. J. Funct.Foods 64, 103652. https://doi.org/10.1016/j.jff.2019.103652.

Huang, C., Peng, X., Pang, D.J., Li, J., Paulsen, B.S., Rise, F., Chen, Y.L., Chen, Z.L., Jia, R. Y., Li, L.X., Song, X., Feng, B., Yin, Z.Q., Zou, Y.F., 2021. Pectic polysaccharide from *Nelumbo nucifera* leaves promotes intestinal antioxidant defense *in vitro* and *in vivo*. Food Funct. 12 (21), 10828–10841. https://doi.org/10.1039/D1FO02354C.

Huang, F., Hong, R., Yi, Y., Bai, Y., Dong, L., Jia, X., Zhang, R., Wang, G., Zhang, M., Wu, J., 2020. *In vitro* digestion and human gut microbiota fermentation of longan pulp polysaccharides as affected by *Lactobacillus fermentum* fermentation. Int. J. Biol. Macromol. 147, 363–368. https://doi.org/10.1016/j.ijbiomac.2020.01.059.

Koh, A., De Vadder, F., Kovatcheva-Datchary, P., Backhed, F., 2016. From dietary fiber to host physiology: short-chain fatty acids as key bacterial metabolites. Cell 165 (6), 1332–1345. https://doi.org/10.1016/j.cell.2016.05.041.

Kong, Q., Zhang, R., You, L., Ma, Y., Liao, L., Pedisic, S., 2021. *In vitro* fermentation characteristics of polysaccharide from *Sargassum fusiforme* and its modulation effects on gut microbiota. Food Chem. Toxicol. 151, 112145 https://doi.org/10.1016/j.fct.2021.112145.

Koropatkin, N.M., Cameron, E.A., Martens, E.C., 2012. How glycan metabolism shapes the human gut microbiota. Nat. Rev. Microbiol. 10 (5), 323–335. https://doi.org/10.1038/nrmicro2746.

Li, W., Wu, D.T., Li, F., Gan, R.Y., Hu, Y.C., Zou, L., 2021. Structural and biological properties of water soluble polysaccharides from lotus leaves: effects of drying techniques. Molecules 26 (15), 4395. https://doi.org/10.3390/molecules26154395.

Li, X., Guo, R., Wu, X., Liu, X., Ai, L., Sheng, Y., Song, Z., Wu, Y., 2020. Dynamic digestion of tamarind seed polysaccharide: indigestibility in gastrointestinal simulations and gut microbiota changes *in vitro*. Carbohydr. Polym. 239, 116194. https://doi.org/10.1016/j.carbpol.2020.116194.

Nicholson, J.K., Holmes, E., Kinross, J., Burcelin, R., Gibson, G., Jia, W., Pettersson, S., 2012. Host-gut microbiota metabolic interactions. Science 336 (6086), 1262–1267. https://doi.org/10.1126/science.1223813.

Slavin, J., 2013. Fiber and prebiotics: mechanisms and health benefits. Nutrients 5 (4), 1417–1435. https://doi.org/10.3390/nu5041417.

Song, Q.Q., Wang, Y.K., Huang, L.X., Shen, M.Y., Yu, Y., Yu, Q., Chen, Y., Xie, J.H., 2021. Review of the relationships among polysaccharides, gut microbiota, and human health. Food Res. Int. 140, 109858 https://doi.org/10.1016/j.foodres.2020.109858.

Song, Y.R., Han, A.R., Lim, T.G., Lee, E.J., Hong, H.D., 2019. Isolation, purification, and characterization of novel polysaccharides from lotus (*Nelumbo nucifera*) leaves and their immunostimulatory effects. Int. J. Biol. Macromol. 128, 546–555. https://doi.org/10.1016/j.ijbiomac.2019.01.131.

Su, A., Ma, G., Xie, M., Ji, Y., Li, X., Zhao, L., Hu, Q., 2019. Characteristic of polysaccharides from *Flammulina velutipes in vitro* digestion under salivary, simulated gastric and small intestinal conditions and fermentation by human gut microbiota. Int. J. Food Sci. Tech. 54 (6), 2277–2287. https://doi.org/10.1111/ijfs.14142.

van der Beek, C.M., Dejong, C.H.C., Troost, F.J., Masclee, A.A.M., Lenaerts, K., 2017. Role of short-chain fatty acids in colonic inflammation, carcinogenesis, and mucosal protection and healing. Nutr. Rev. 75 (4), 286–305. https://doi.org/10.1093/nutrit/nuw067.

Wang, Y., Yao, W.F., Li, B., Qian, S.Y., Wei, B.B., Gong, S.Q., Wang, J., Liu, M.Y., Wei, M. J., 2020. Nuciferine modulates the gut microbiota and prevents obesity in high-fat diet-fed rats. Exp. Mol. Med. 52 (12), 1959–1975. https://doi.org/10.1038/s12276-020-00534-2.

Wang, Z.Y., Cheng, Y., Zeng, M.M., Wang, Z.J., Qin, F., Wang, Y.Z., Chen, J., He, Z.Y., 2021. Lotus (*Nelumbo nucifera* Gaertn.) leaf: a narrative review of its phytoconstituents, health benefits and food industry applications. Trends Food Sci. Technol. 112, 631–650. https://doi.org/10.1016/j.tifs.2021.04.033.

Wu, D.T., Feng, K.L., Huang, L., Gan, R.Y., Hu, Y.C., Zou, L., 2021a. Deep eutectic solvent-assisted extraction, partially structural characterization, and bioactivities of acidic polysaccharides from lotus leaves. Foods 10 (10), 2330. https://doi.org/10.3390/foods10102330.

Wu, D.T., Fu, Y., Guo, H., Yuan, Q., Nie, X.R., Wang, S.P., Gan, R.Y., 2021b. *In vitro* simulated digestion and fecal fermentation of polysaccharides from loquat leaves: dynamic changes in physicochemical properties and impacts on human gut microbiota. Int. J. Biol. Macromol. 168, 733–742. https://doi.org/10.1016/j.ijbiomac.2020.11.130.

Wu, D.T., He, Y., Fu, M.X., Gan, R.Y., Hu, Y.C., Peng, L.X., Zhao, G., Zou, L., 2022. Structural characteristics and biological activities of a pectic-polysaccharide from okra affected by ultrasound assisted metal-free Fenton reaction. Food Hydrocolloid 122, 107085. https://doi.org/10.1016/j.foodhyd.2021.107085.

Wu, D.T., Nie, X.R., Gan, R.Y., Guo, H., Fu, Y., Yuan, Q., Zhang, Q., Qin, W., 2021c. *In vitro* digestion and fecal fermentation behaviors of a pectic polysaccharide from okra (*Abelmoschus esculentus*) and its impacts on human gut microbiota. Food Hydrocolloid 114, 106577. https://doi.org/10.1016/j.foodhyd.2020.106577.

Wu, D.T., Yuan, Q., Guo, H., Fu, Y., Li, F., Wang, S.P., Gan, R.Y., 2021d. Dynamic changes of structural characteristics of snow chrysanthemum polysaccharides during *in vitro* digestion and fecal fermentation and related impacts on gut microbiota. Food Res. Int. 141, 109888 https://doi.org/10.1016/j.foodres.2020.109888.

Xu, S.Y., Aweya, J.J., Li, N., Deng, R.Y., Chen, W.Y., Tang, J., Cheong, K.L., 2019. Microbial catabolism of *Porphyra haitanensis* polysaccharides by human gut microbiota. Food Chem. 289, 177–186. https://doi.org/10.1016/j.foodchem.2019.03.050.

Xu, S.Y., Chen, X.Q., Liu, Y., Cheong, K.L., 2020. Ultrasonic/microwave-assisted extraction, simulated digestion, and fermentation *in vitro* by human intestinal flora of polysaccharides from *Porphyra haitanensis*. Int. J. Biol. Macromol. 152, 748–756. https://doi.org/10.1016/j.ijbiomac.2020.02.305.

Yuan, Q., Lin, S., Fu, Y., Nie, X.R., Liu, W., Su, Y., Han, Q.H., Zhao, L., Zhang, Q., Lin, D. R., Qin, W., Wu, D.T., 2019. Effects of extraction methods on the physicochemical characteristics and biological activities of polysaccharides from okra (*Abelmoschus esculentus*). Int. J. Biol. Macromol. 127, 178–186. https://doi.org/10.1016/j.ijbiomac.2019.01.042.

Zeng, Z., Xu, Y., Zhang, B., 2017. Antidiabetic activity of a lotus leaf selenium (Se)-polysaccharide in rats with gestational diabetes mellitus. Biol. Trace Elem. Res. 176 (2), 321–327. https://doi.org/10.1007/s12011-016-0829-6.

Zhang, L., Tu, Z.C., Wang, H., Kou, Y., Wen, Q.H., Fu, Z.F., Chang, H.X., 2015. Response surface optimization and physicochemical properties of polysaccharides from *Nelumbo nucifera* leaves. Int. J. Biol. Macromol. 74, 103–110. https://doi.org/10.1016/j.ijbiomac.2014.11.020.

Zhang, X., Liu, Y., Chen, X.Q., Aweya, J.J., Cheong, K.L., 2020. Catabolism of *Saccharina japonica* polysaccharides and oligosaccharides by human fecal microbiota. LWT - Food Sci. Technol. (Lebensmittel-Wissenschaft -Technol.) 130, 109635. https://doi.org/10.1016/j.lwt.2020.109635.